

Noise Resilient Segmentation of Oil Spills in SAR Imagery

Ayesha Jabbar* and Junaid Mir²

¹Department of Electrical Engineering, University of Engineering and Technology, Taxila, Pakistan

²Department of Electrical Engineering, University of Engineering and Technology, Taxila, Pakistan

*(ayeshajabbar49@gmail.com)

(Received: 25 May 2025, Accepted: 10 June 2025)

(1st International Conference on Pioneer and Academic Research ICPAR 2025, June 13-14, 2025)

ATIF/REFERENCE: Jabbar, A. & Mir, J. (2025). Noise Resilient Segmentation of Oil Spills in SAR Imagery. *International Journal of Advanced Natural Sciences and Engineering Researches*, 9(6), 174-183.

Abstract – Oil spills are one of the most detrimental environmental disasters, that often cause a serious threat to aquatic life, coastal habitats, and human livelihoods. Timely detection and accurate segmentation of oil spills are therefore critical for effective response and mitigation. This research particularly aims to detect and segment oil spills from low-quality SAR images using the SAR Oil Spill (SOS) dataset from ALOS and Sentinel-1A satellites covering spill-affected areas in the Gulf of Mexico and the Persian Gulf respectively. SAR images are inherently affected by various types of noise, such as speckle and thermal noise, as well as distortions like RF interference and motion artifacts, which complicate accurate analysis. To address these challenges, a multi-phase methodology was adopted. In the first phase, a baseline U-Net model was implemented on raw SAR imagery. The second phase integrated preprocessing techniques, specifically Fast & Flexible Denoising CNN (FFD-Net) for noise removal and unsharp masking for image sharpening, before U-Net-based segmentation. The third phase introduced an optimized U-Net model with a deeper and more lightweight architecture and improved training strategies, combined with the earlier preprocessing steps. Experimental evaluations demonstrated that the optimized model with preprocessing delivered the highest detection accuracy and lowest false positive rates, indicating its strong potential for integration into real-time, satellite-based oil spill monitoring systems.

Keywords – Convolutional neural networks (CNNs), Phased Array L-band Synthetic Aperture Radar (PALSAR), Advanced Land Observing Satellite (ALOS), SAR Oil Spill (SOS), Oil Spill, U-NET.

I. INTRODUCTION

Oil spills represent one of the most devastating forms of marine pollution, introducing large quantities of petroleum hydrocarbons into aquatic environments through accidental releases or deliberate discharges [1], [3], [7]. These catastrophic events cause profound and long-lasting damage to marine ecosystems, often extending beyond the immediate vicinity of the spill. The released petroleum compounds create a physically suffocating layer on the water surface that impedes oxygen exchange between the atmosphere and water column, while simultaneously releasing toxic components that directly poison aquatic life. The ecological consequences are multifaceted and severe, including mass mortality of seabirds through hypothermia and ingestion of oil, destruction of marine mammal insulation and buoyancy, and decimation of fish populations through gill damage and developmental abnormalities [4]. The timely detection and monitoring of oil spills

are crucial for implementing effective containment measures and mitigating ecological impact. Synthetic Aperture Radar (SAR) has emerged as an indispensable remote sensing technology for oil spill monitoring due to its ability to provide high-resolution imagery under all-weather conditions and during both day and night operations. Oil spills appear as distinctive dark spots in SAR imagery because they dampen capillary waves on the sea surface, thereby suppressing backscattered radio waves [10]. However, the effectiveness of SAR-based oil spill detection faces significant challenges, primarily due to the presence of speckle noise—a multiplicative noise inherent to SAR imagery—and look-alikes such as low wind areas, algal blooms, and wave shadows, which can be misidentified as oil spills [10, 13].

Effective preprocessing techniques to address speckle noise represent a critical foundation for any reliable oil spill detection system. Traditional noise reduction approaches often sacrifice important spatial details or diminish resolution quality. Addressing these limitations, researchers have developed innovative deep learning solutions like the Image De-speckling Convolutional Neural Network (ID-CNN), which employs specialized convolutional architectures with batch normalization and custom residual layers to effectively manage speckle while preserving crucial structural information [5]. These advanced approaches have demonstrated measurable improvements over conventional de-speckling methods in both synthetic and authentic SAR imagery applications.

The integration of deep learning methodologies has transformed SAR image analysis for oil spill detection. The Oil Spill Convolutional Network (OSNet), developed from VGG-16 architecture fundamentals, significantly outperforms traditional machine learning techniques [9]. This performance enhancement stems from the network's capacity to autonomously develop discriminative features directly from training data, eliminating the need for manually engineered feature sets that characterize conventional techniques.

Complementary research directions have explored random forest classification systems with optimized feature spaces that incorporate multidimensional attributes spanning statistics, shape parameters, fractal geometry principles, textural elements, and gradient-based characteristics, achieving detection accuracy rates approaching 90% [11]. Semantic segmentation frameworks based on encoding-decoding network architectures like Deeplabv3+ have implemented novel loss functions derived from Gibbs distribution principles to establish meaningful semantic relationships between classification categories [12]. These approaches have yielded superior performance in terms of intersection over union metrics and global accuracy while minimizing computational overhead.

Recognizing the constraints of remote sensing platforms, particularly nano and micro-satellites with limited processing capabilities and strict power requirements, researchers have developed streamlined CNN architectures optimized for resource-constrained environments [13]. While these compact models may not advance absolute accuracy benchmarks, they deliver substantial benefits in operational efficiency, including faster inference and training cycles, reduced data transmission requirements, and compatibility with onboard processing systems for real-time monitoring applications.

Research has increasingly incorporated polarimetric SAR (PolSAR) data, which provides enriched scattering information including phase components and polarimetric decomposition parameters beyond standard amplitude measurements [17]. Integrating these expanded data dimensions into advanced frameworks such as modified DeepLabv3+ models with ResNet-101 backbone structures has produced superior results in capturing fine-scale oil spill boundaries and achieving precise segmentation outcomes. Recent innovations include adaptive detection networks featuring dynamic convolution modules and boundary constraint mechanisms, which have demonstrated accuracy improvements as compared to previous methodologies [21].

In this work, we propose an improved oil spill detection model for Synthetic Aperture Radar (SAR) images that successfully tackles two important issues: look-alike discrimination and speckle noise interference. We used contrast enhancement methods including Contrast Limited Adaptive Histogram Equalization (CLAHE) and unsharp masking in conjunction with FFD-Net, a deep learning-based denoising tool, to reduce the inherent noise in SAR images. The clarity and feature differentiation of the

images were much enhanced by these preprocessing processes. We created a lightweight, optimized U-Net architecture specifically designed to minimize memory utilization and computational complexity while preserving good speed for the segmentation task. With a remarkable segmentation accuracy of 90.53%, this model proved to be successful at precisely detecting oil spills in poor-quality SAR pictures. Our method improves the accuracy and dependability of oil spill detection systems and provides a workable alternative for managing marine pollution and real-time environmental monitoring with lower computational complexity.

The remaining sections of this paper are organized as follows. Section II describes the dataset used and its collection procedure. Section III details our proposed methodology including the network architecture and training process incorporating the preprocessing methods used to refine SAR imagery required for training neural networks,. Section IV presents comprehensive analysis results of the segmented oil spill images generated by our proposed optimized model, along with performance metrics and comparative tables. Finally, Section V offers conclusions, discusses implications of our findings, and suggests directions for future research in this field.

II. MATERIALS AND METHOD

The segmentation of oil spills from SAR images in our research project is structured into the following distinct phases:

- Step A: Annotated Dataset Collection
- Step B: Dataset Pre-processing
- Step C: Training Model
- Step D: Evaluation of the Model

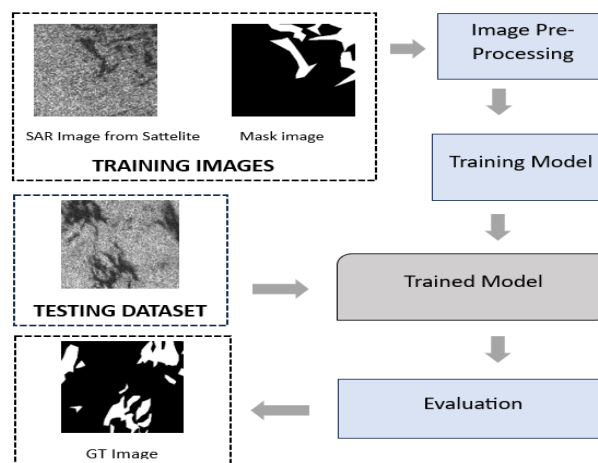


Figure 1 : Block Diagram of Methodology

A. Datasets

This section deals with the SAR Oil Spill (SOS) dataset [16]. It was created and distributed by the URSmart group at the China University of Geosciences, Wuhan by Zhu et al. in 2022. SOS dataset is the most complex and variable dataset for oil spill detection widely used for research and academia. The dataset was made by 21 images initially, 14 images from a Japanese satellite ALOS(Advanced Land Observing Satellite) and 7 images from Sentinel-1 Satellite [20]. In order to enhance the model performance to detect oil spills accurately various data augmentation techniques including cropping, rotating, flipping and adding noise to those images were done such that the total number of images in that dataset was increased. Those 21 images multiplied in number and the dataset includes 6456 images of 416×416 pixels and on further processing dataset, a total of 8070 images of 256×256 pixels was created [8], [16].

The SOS dataset used in this study comprises SAR images from two major oil spill events. The first is from the April 2010 Deepwater Horizon disaster in the Gulf of Mexico, where the oil slick spanned 11,520 km² [5]. This portion includes 3,887 L-band SAR images from the PALSAR sensor on Japan's ALOS satellite, with 3,101 used for training and 776 for testing [20]. The second dataset segment features 4,193 SAR images from ESA's Sentinel-1 satellite, capturing an oil spill off Kuwait's coast near Al Khiran in the Persian Gulf on August 11, 2017 [8]. It consists of 3,354 for training and 839 for testing. This dataset was proposed by Q. Zhu in 2021, and supports academic and research applications in oil spill detection [16].

B. Data Pre-Processing

The SAR images used in this study are sourced from the SOS dataset, which predominantly comprises low-quality imagery affected by various forms of noise particularly speckle noise. To enhance image quality and ensure reliable feature extraction, a comprehensive preprocessing pipeline was implemented. Initially, (FFD-Net) Fast and Flexible Denoising CNN based model, designed for image denoising tasks effectively suppress speckle noise and Gaussian noise while preserving critical structural information. The process starts with data preparation, where clean images are randomly cropped into small patches (64×64). Noise is then added using either Gaussian noise (additive) or speckle noise (multiplicative), simulating real-world conditions. A noise level map, which encodes the noise intensity, is created and used as an auxiliary input. This noise-aware approach helps the model generalize to varying noise conditions. The FFD-Net architecture consists of an input layer that accepts both the noisy image and its corresponding noise level map. These are concatenated and passed through convolutional layers followed by batch normalization and ReLU activation for feature extraction. A series of residual blocks then refines the features while preserving contextual information. The output layer predicts the noise component, which is subtracted from the input image during inference to produce the denoised result. This makes the training efficient and adaptable to various noise distributions.

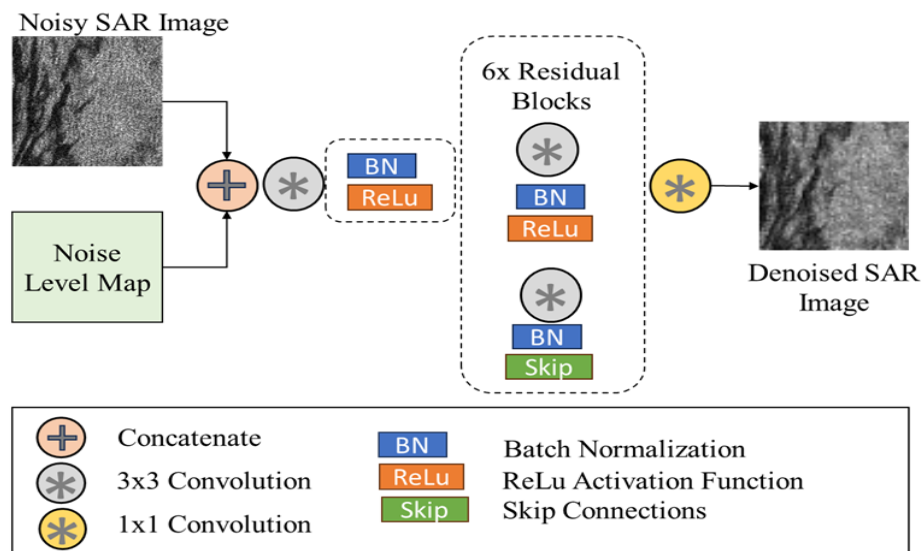


Figure 2 : FFD-Net Architecture

For further preprocessing the images a technique known as CLAHE (Contrast Limited Adaptive Histogram Equalization) was applied to each image to improve local contrast and highlight subtle variations in intensity, which are often critical for distinguishing oil spills from background water surfaces. Finally, the images were processed using Unsharp Masking, which is an image sharpening technique that accentuates edges and enhances fine spatial details by amplifying high-frequency components. Together, these preprocessing steps created an optimized input set that facilitated the model in learning more discriminative features [18]. The preprocessed images were normalized and resized before being input to

the proposed architecture, resulting in more precise and reliable segmentation outputs across diverse SAR imaging scenarios.

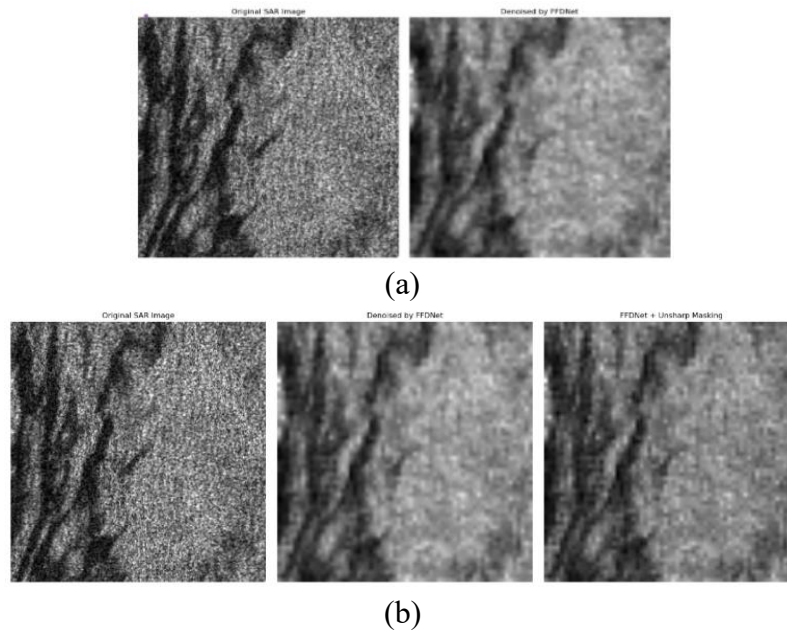


Figure 3 : (a) SAR image denoised with FFD-Net (b) SAR image denoised by FFD-Net and sharpened by Unsharpmasking

C. Optimized U-Net

The U-Net architecture was introduced by Olaf Ronneberger et al. in 2015 particularly for biomedical image segmentation, under the paper titled “U-Net: Convolutional Networks for Biomedical Image Segmentation” which was presented at the International Conference on Medical Image Computing and Computer-Assisted Intervention (MICCAI) [2]. The model was specifically designed to perform pixel-wise segmentation with high accuracy, even on limited datasets. It is a fully convolutional neural network (FCN) with an encoder decoder blocks making a “U” shaped structure. Encoder encodes and downsamples the image context using convolution layer and pooling layer while decoder upsamples using convolution. A thorough preprocessing pipeline was put in place to overcome the challenges of noise in SAR images. FFD-Net was used to reduce noise effectively, and CLAHE and unsharp masking were used to improve contrast and edge clarity, which in turn improved segmentation accuracy.

A lightweight and effective version of the traditional U-Net architecture is designed in this work for oil spill segmentation task. This optimized U-Net is especially well-suited for deployment in contexts with limited resources because it strikes a compromise between segmentation accuracy and computing efficiency. The model utilizes a streamlined encoder-decoder structure with skip connections, it processes greyscale SAR images of $256 \times 256 \times 1$ and produces binary segmentation masks with the same dimensions. Key optimizations include reduced filter sizes in the encoder (32, 64, and 128 filters) and decoder paths, strategic dropout regularization (ranging from 0.1 to 0.3), and the use of nearest-neighbour upsampling to minimize computational overhead. The bottleneck layer gathers abstract characteristics necessary for precise segmentation by using 256 filters and a greater dropout rate. For efficient feature learning, each convolutional block consists of two 3×3 convolutional layers with batch normalization and ReLU activation. Fine spatial features are preserved through the use of skip connections between the encoder and decoder stages. The final segmentation mask is produced via a 1×1 convolution with sigmoid activation at the output layer.

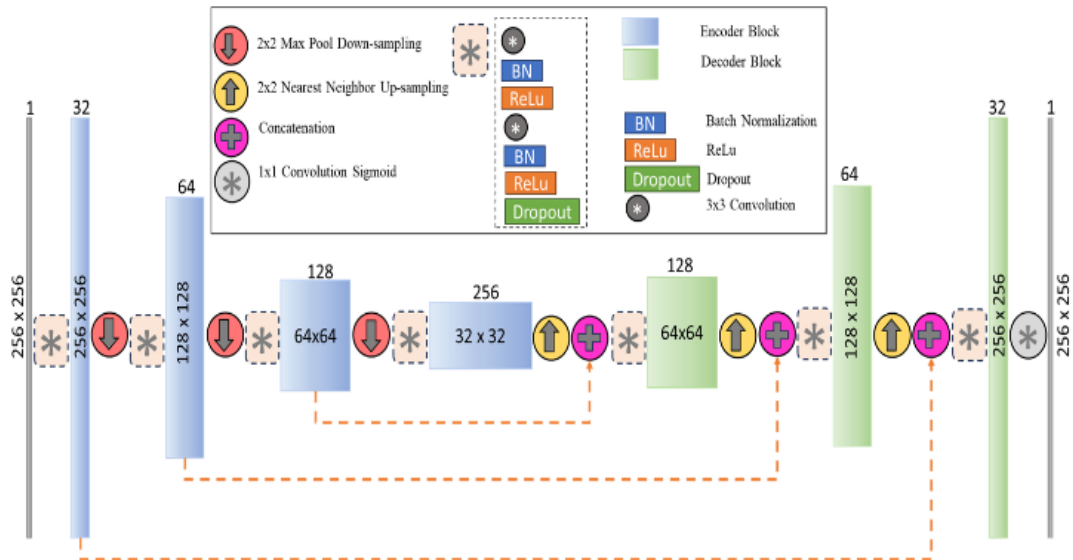


Figure 4 : Optimized U-NET Architecture

To effectively handle class imbalance, the model employs a hybrid loss function combining Dice loss and focal loss. Additionally, the FastDataGenerator class facilitates real-time data augmentation on grayscale images and masks, enabling accelerated and diverse training. This entire pipeline is tailored for deployment in resource-constrained environments, ensuring high segmentation accuracy (90.53%) and faster convergence without the need for high-end computational infrastructure. The proposed methodology exemplifies how deep learning can be adapted for practical, real-world SAR image analysis, advancing the reliability and accessibility of oil spill detection systems.

III. RESULTS

The model proposed in this article is optimized U-Net with FFD-Net preprocessing as it requires less computational complexity with satisfying results. The training process uses 30 epochs with early stopping after 10 epochs without improvement, which significantly reduces training time while maintaining performance. The batch size is set to 8, which is smaller than typical implementations to accommodate lower memory requirements on standard hardware. Adam optimizer with an initial learning rate of 1e-3 is used, allowing the model to fine-tune effectively.

A) Evaluation Criteria

The segmentation performance was evaluated using key metrics suited for imbalanced datasets like oil spill detection in SAR images. Primary metrics included F1 Score and Intersection over Union (IoU) for assessing pixel-level classification accuracy. Additional metrics Accuracy, Precision, Recall (Sensitivity), and Specificity—were used to evaluate various aspects of model performance, such as detecting true oil spills, avoiding false positives, and correctly identifying non-oil regions. Evaluations were performed on three model variants: baseline U-Net, U-Net with preprocessing (FFD-Net and unsharp masking), and an optimized U-Net with pre-processing. These were tested on both PALSAR and Sentinel-1 datasets to ensure robustness and generalizability.

B) Experimental Analysis

The experimental results demonstrate the effectiveness and generalizability of the proposed lightweight U-Net model for oil spill segmentation using SAR imagery. Training on the Sentinel-1 dataset yielded promising results, with a final training Dice coefficient of 0.7528 and validation Dice coefficient of 0.7586, indicating strong overlap between predicted and ground truth masks. The loss curves steadily decline, reflecting consistent learning without overfitting, while the Dice coefficient improves across epochs. Evaluation metrics on the Sentinel-1 test set report an accuracy of 83.70%, F1-score of 77.98%, and IoU

of 63.91%, affirming the model's reliable segmentation capability. High recall (83.13%) and specificity (84.00%) further indicate balanced sensitivity to oil spill detection and correct classification of non-spill areas. Notably, cross-corpora testing on the PALSAR dataset highlights the model's robustness, achieving an accuracy of 90.53%, despite a lower IoU (56.52%) due to domain shift. The F1-score remains reasonably high at 72.22%, suggesting the model can generalize across datasets without fine-tuning.

The proposed optimized lightweight U-Net architecture shows promising results as shown in Figure 6. The loss curves indicate a consistent decrease in training loss from approximately 0.21 to 0.16 over 25 epochs, suggesting effective model optimization. While the validation loss exhibited greater variability with notable fluctuations reaching peaks of 0.36 and 0.29 in early epochs and 0.27 around epoch 10 it ultimately stabilized near 0.18, indicating reasonable generalization capability. The Dice coefficient metrics reveal substantial improvement during training, with the coefficient rising from initial values around 0.65 to approximately 0.75 by epoch 25 for both training and validation sets, despite the validation metric showing more pronounced oscillations throughout.

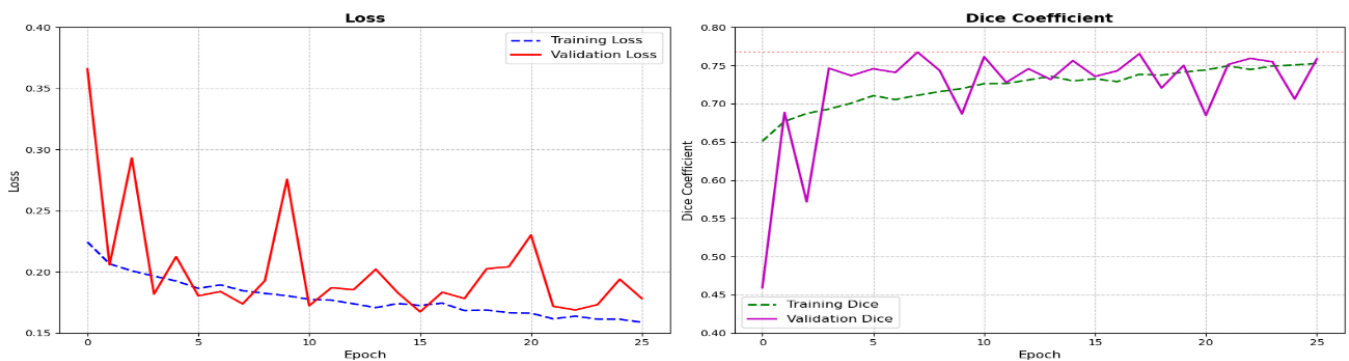


Figure 5 : Loss curve and Dice Coefficient for Sentinel-1

The training results using the PALSAR dataset illustrate the robust performance and stability of the proposed optimized U-Net model. Over 30 epochs, the training and validation losses converge smoothly, stabilizing around 0.15, while the Dice coefficient reaches 0.7572 for training and 0.7520 for validation, indicating consistent learning and minimal overfitting. The evaluation on the PALSAR test set yields a high accuracy of 91.70%, with a F1-score of 75.19% and an IoU of 60.25%, demonstrating precise delineation of oil spill regions. The model maintains a strong balance between precision (75.54%) and recall (74.84%), suggesting it can reliably detect true oil spills while minimizing false alarms. Additionally, a specificity of 95.11% confirms its effectiveness in correctly identifying non-spill areas.

To assess the model's generalization capabilities, cross-corpora testing was conducted on the Sentinel-1 dataset. Remarkably, the model achieved an accuracy of 83.79% and F1-score of 78.60%, outperforming its native-domain performance in terms of segmentation quality. The IoU reached 64.74%, and recall peaked at 85.73%, indicating that the model effectively adapts to different SAR sources. While precision dropped slightly to 72.56%, the overall trade-off remains favorable. These outcomes confirm that the trained U-Net model retains strong cross-domain generalizability, making it suitable for real-world deployment in diverse satellite imaging scenarios without retraining.

The U-Net architecture trained on PALSAR satellite data exhibited exceptional convergence characteristics, as evidenced by the training curves in Figure 7. The loss function demonstrated rapid initial descent, stabilizing at approximately 0.15 by the final epoch, with minimal divergence between training and validation losses throughout the training process. The Dice coefficient metrics showed remarkable improvement, climbing from initial values below 0.4 to consistently above 0.75 for both training and

validation sets by epoch 10, with the training Dice coefficient showing steady improvement while the validation metric exhibited occasional fluctuations yet maintained a positive trajectory.

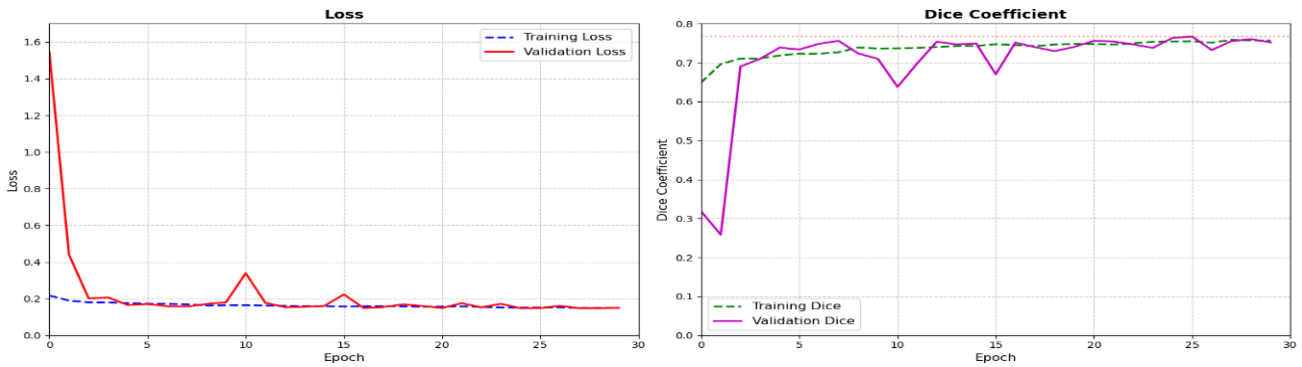


Figure 6 : Loss curve and Dice Coefficient for PALSAR

These findings validate that the proposed lightweight model delivers competitive performance across different SAR domains, all while maintaining low computational requirements making it practical for real-time or edge deployment where high-end GPUs are unavailable.

Table 1 : Comparison of Implemented Models

Models	Satellite	F1-Score		IOU	
		Palsar	Sentinel-1	Palsar	Sentinel-1
U-NET	Palsar	27.92%	23.60%	16.2%	34.81%
	Sentinel-1	51.27%	48.03%	25.34%	40.50%
U-NET+ FFD-Net	Palsar	75.37%	70.57%	60.48%	54.45%
	Sentinel-1	78.31%	72.38%	64.36%	56.71%
Optimized U-NET + FFD-Net	Palsar	75.19%	72.22%	60.25%	56.52%
	Sentinel-1	78.60%	77.98%	64.74%	63.91%

The optimized U-Net model, combined with FFD-Net denoising and unsharp masking, achieved the highest performance on both PALSAR and Sentinel-1 datasets, with F1 scores of 78.60% and 77.98%, and IoU values of 64.74% and 63.91%, respectively. However, the performance gain over the previously preprocessed model was marginal, suggesting that preprocessing contributes more significantly to improvement than architectural optimization. Visual results further confirm the model's effectiveness in accurately segmenting oil spills from noisy, low-contrast SAR images, highlighting the crucial role of the preprocessing pipeline in enhancing segmentation quality.

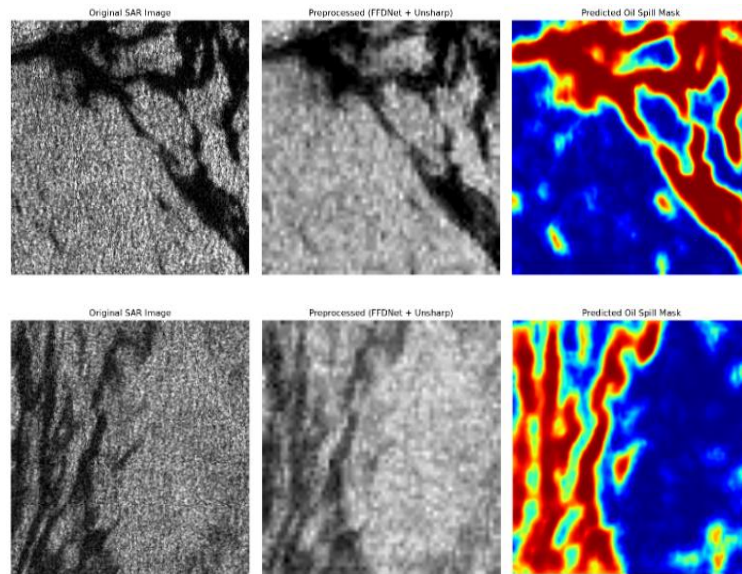


Figure 7 : Visual Interpretation of Oil Spill Segmentation

IV. DISCUSSION

The results demonstrate the value of a simplified preprocessing and segmentation pipeline designed specifically for SAR image analysis, especially when it comes to oil spill detection. By reducing speckle noise, which is frequently present in SAR imaging, the incorporation of FFD-Net, a deep learning-based denoising model, greatly improved the quality of input data for further processing. Clearer demarcation of oil spill borders was ensured by the preprocessing stage, which further enhanced local contrast and edge sharpness in conjunction with Contrast Limited Adaptive Histogram Equalization (CLAHE) and unsharp masking. Together, these improvements produced segmentation results that were more accurate. In order to overcome computational and memory constraints without sacrificing accuracy, an optimized U-Net architecture was adopted. This architecture was created with a lower filter depth, fewer convolutional stages, and effective upsampling. This lightweight model is appropriate for deployment in resource-constrained contexts since it consistently produced great performance with fewer parameters. The optimized version confirmed the feasibility of U-Net for real-time or embedded applications by achieving similar or better segmentation results with less inference time than typical U-Net implementations. The importance of task-specific architectural and preprocessing decisions in developing SAR-based oil spill monitoring is highlighted by these findings.

V. CONCLUSION

In this study, a comprehensive evaluation of oil spill segmentation in SAR images was conducted using various configurations of the U-Net model, enhanced by preprocessing techniques such as Unsharp Masking, CLAHE and FFD-Net denoising. The performance was assessed using standard evaluation metrics including precision, recall, specificity, F1-score, and IoU, ensuring a thorough analysis of both detection accuracy and segmentation quality on both PALSAR and Sentinel-1 datasets. The results demonstrate that preprocessing significantly improves model performance, and further optimization of the U-Net architecture yields additional gains. The consistent outcomes across both PALSAR and Sentinel-1 datasets highlight the robustness and generalizability of the proposed approach. These findings suggest that integrating image enhancement with an optimized deep learning model can provide a reliable solution for accurate oil spill detection and segmentation in real-world SAR data applications.

ACKNOWLEDGMENT

The author would acknowledge Qiqi Zhu and others for making and sharing the SOS annotated dataset of PALSAR and Sentinel-1 publicly available, which played a crucial role in the experimental analysis. We also acknowledge the contributions of colleagues and mentors who provided valuable insights and guidance

during the course of this work.

REFERENCES

- [1] Topouzelis, K., Karathanassi, V., Pavlakis, P., & Rokos, D. (2007). Detection and discrimination between oil spills and look-alike phenomena through neural networks. *ISPRS Journal of Photogrammetry and Remote Sensing*, 62(4), 264–270.
- [2] Ronneberger, O., Fischer, P., & Brox, T. (2015). U-net: Convolutional networks for biomedical image segmentation. In *Proceedings of the 18th International Conference on Medical Image Computing and Computer-Assisted Intervention (MICCAI)* (Vol. 9351, pp. 234–241). Munich, Germany: Springer.
- [3] Yu, F., Sun, W., Li, J., Zhao, Y., Zhang, Y., & Chen, G. (2017). An improved Otsu method for oil spill detection from SAR images. *Oceanologia*, 59(3), 311–317. <https://doi.org/10.1016/j.oceano.2017.03.005>
- [4] Li, Y., Zhang, Y., Yuan, Z., Guo, H., Pan, H., & Guo, J. (2018). Marine oil spill detection based on the comprehensive use of polarimetric SAR data. *Sustainability*, 10(12), 4408. <https://doi.org/10.3390/su10124408>
- [5] Carvalho, G. D. A., Minnett, P. J., De Miranda, F. P., Landau, L., & Paes, E. T. (2017). Exploratory data analysis of synthetic aperture radar (SAR) measurements to distinguish the sea surface expressions of naturally-occurring oil seeps from human-related oil spills in Campeche Bay (Gulf of Mexico). *ISPRS International Journal of Geo-Information*, 6, 379.
- [6] Wang, P., Zhang, H., & Patel, V. M. (2017). SAR image despeckling using a convolutional neural network. *IEEE Signal Processing Letters*, 24(12), 1763–1767.
- [7] Raeesi, A., Akbarizadeh, G., & Mahmoudi, A. (2018). Combined method of an efficient cuckoo search algorithm and nonnegative matrix factorization of different Zernike moment features for discrimination between oil spills and lookalikes in SAR images. *IEEE Journal of Selected Topics in Applied Earth Observations and Remote Sensing*, 11(11), 4193–4205.
- [8] Chaturvedi, S. K., Banerjee, S., & Lele, S. (2020). An assessment of oil spill detection using Sentinel-1 SAR-C images. *Journal of Ocean Engineering and Science*, 5(2), 116–135. <https://doi.org/10.1016/j.joes.2019.09.004>
- [9] Zeng, K., & Wang, Y. (2020). A deep convolutional neural network for oil spill detection from spaceborne SAR images. *Remote Sensing*, 12(6), 1015. <https://doi.org/10.3390/rs12061015>
- [10] Magri, S., Vairo, T., Reverberi, A. P., & Fabiano, B. (2021). Oil spill identification and monitoring from Sentinel-1 SAR satellite earth observations: A machine learning approach. *Chemical Engineering Transactions*, 86, 379–384. <https://doi.org/10.3303/CET218606>
- [11] Conceição, M. R. A., de Mendonça, L. F. F., Lentini, C. A. D., da Cunha Lima, A. T., Lopes, J. M., de Vasconcelos, R. N., Gouveia, M. B., & Porsani, M. J. (2021). SAR oil spill detection system through random forest classifiers. *Remote Sensing*, 13(11), 2044.
- [12] Kong, Y., Liu, Y., Yan, B., Leung, H., & Peng, X. (2021). A novel DeepLabV3+ network for SAR imagery semantic segmentation based on the potential energy loss function of Gibbs distribution. *Remote Sensing*, 13(3), 454.
- [13] Diana, L., Xu, J., & Fanucci, L. (2021). Oil spill identification from SAR images for low power embedded systems using CNN. *Remote Sensing*, 13, 3606.
- [14] Wang, X., Liu, J., Zhang, S., Deng, Q., Wang, Z., Li, Y., & Fan, J. (2021). Detection of oil spill using SAR imagery based on AlexNet model. *Computational Intelligence and Neuroscience*, 2021, Article ID 4812979, 1–14.
- [15] Fan, Y., Rui, X., Zhang, G., Yu, T., Xu, X., & Poslad, S. (2021). Feature merged network for oil spill detection using SAR images. *Remote Sensing*, 13, 3174.
- [16] Zhu, Q., Zhang, Y., Li, Z., Yan, X., Guan, Q., Zhong, Y., Zhang, L., & Li, D. (2021). Oil spill contextual and boundary-supervised detection network based on marine SAR images. *IEEE Transactions on Geoscience and Remote Sensing*, 2021.
- [17] Ma, X., Xu, J., Wu, P., & Kong, P. (2022). Oil spill detection based on deep convolutional neural networks using polarimetric scattering information from Sentinel-1 SAR images. *IEEE Transactions on Geoscience and Remote Sensing*, 60, Article ID 4204713. <https://doi.org/10.1109/TGRS.2021.3126175>
- [18] Mahmoudi Ghara, F., Shokouhi, S. B., & Akbarizadeh, G. (2022). A new technique for segmentation of the oil spills from synthetic-aperture radar images using convolutional neural network. *IEEE Journal of Selected Topics in Applied Earth Observations and Remote Sensing*, 15, 8834–8844.
- [19] Fan, J., & Liu, C. (2023). Multitask GANs for oil spill classification and semantic segmentation based on SAR images. *IEEE Journal of Selected Topics in Applied Earth Observations and Remote Sensing*, 16, 2532–2546.
- [20] Li, C., Yang, Y., Yang, X., Chu, D., & Cao, W. (2024). A novel multi-scale feature map fusion for oil spill detection of SAR remote sensing. *Remote Sensing*, 16, 1684.
- [21] Song, D., Huang, Q., Gao, H., Wang, B., Zhang, J., & Chen, W. (2024). Adaptive oil spill detection network for scene-based PolSAR data using dynamic convolution and boundary constraints. *International Journal of Applied Earth Observation and Geoinformation*, 130.